NTU Journal of Engineering and Technology (ICSDT2025) special issue
DOI: https://doi.org/10.56286/ntujet.icsdt2025

IRAQI Academic Scientific Journals

P-ISSN: 2788-9971 E-ISSN: 2788-998X
NTU Journal of Engineering and Technology
Available online at: https://journals.ntu.edu.iq/index.php/NTU-JET/index

Analysis of Voltage Performance and Temperature Effects in a Tracking Floating Photovoltaic System

Musa Anwar Omar[1], Rana H. A. Zubo[1], Hussein Fadhel[1]
[1,2,3]Electronic and Control Eng. Department, Technical Engineering College /Kirkuk, 36001, Northern Technical University, Mosul, Iraq
musaa.anwr@ntu.edu.iq, r.h.a.zubo@ntu.edu.iq, h.fadil@ntu.edu.iq,

Article Informations

Received: 15-03- 2025,
Accepted: 28-04-2025,
Published online: 01-03-2026

Corresponding author:
Name:Musa Anwar Omar
Affiliation: Northern Technical University
Email:musaa.anwr@ntu.edu.iq

Key Words:
Floating PV,
Sun tracking,
Optimization.

A B S T R A C T

This study examines a one axis sun tracking floating photovoltaic system located in Northern Iraq (35.407533°N, 44.413411°E). While fixed floating PV systems have been studied extensively, the integration of tracking mechanisms with floating installations remains underexplored, particularly in regions with high solar potential and significant water resources like Iraq. the floating platform holds a system with a 120W photovoltaic module attached to it that can track ±45° horizontally. A mathematical model based on the voltage generated was developed by taking temperature effects, tracking angle and water-surface effects. The collected performance data showed remarkable benefits from tracking implementation with voltage gains above 100% during early morning hours. While, Daily energy yields showed improvements of 22.5 ± 0.7%. The developed mathematical model predicted values at all operating conditions with an accuracy of 96-98% with RMSE of 0.15V and 0.11V for fixed and tracking, respectively. Temperature analysis revealed that the optimal cell temperature range is 25-30°C. The floating configuration kept the temperature of the cell 2.8°C lower than that of an equivalent ground configuration. The tracking system performed more efficiently than the fixed system and showed a maximum system efficiency of 10.51% compared to 9.67% for the fixed system. The results show that tracking systems in floating photovoltaic applications is effective and provide a foundation for further future optimization.

1. Introduction

Floating photovoltaic (FPV) systems are a relatively new approach of deploying renewable energy that attempts to give a balanced solution to land use and energy efficiency problems. These systems demonstrated interesting benefits, including up to 12.5% increase in energy yield compared to traditional ground-mounted installations due to natural cooling [1,2]. The global installed capacity of the technology is growing rapidly, increasing from 1.1 GW in 2018 to an estimated 4.8 GW at the end of 2021 [3]. With water being an important resource and a solar potential of 5.6-6.8 kWh/m²/day, Iraq can be a viable location for the implementation of FPV [4]. The country has reservoirs, canals, and hydro dams suitable for installing FPV of about 20,000 hectares water surface area. This potential is very important since Iraq aims to have alternative energy sources and to cut carbon emissions as well.

Fixed FPV installations are used widely, however, floating with tracking presents a different paradigm and unique opportunity and new challenges. Traditional solar tracking technology used for ground-mounted installations increases energy yield by anywhere between 20% and 40% [5]. however, one of the biggest challenges related to using Traditional solar tracking in floater designs is the mechanical and stability aspects. The water surface poses unique problems for tracking systems due to waves, wind and corrosion but also benefits from cooling which could improve efficiency.

The previous research has focused mainly on fixed floating installations or land-based tracking systems, leaving a gap in knowledge about the performance of tracking mechanisms for floating applications. Limited research has looked into the combined effect of cooling provided by water and optimization of tracking. This is especially true of a region with high-solar radiation and high variation in ambient temperature such as Iraq The thermal behavior of FPV systems with tracking capabilities remains a topic where further research is needed, especially in the context of varying environmental conditions [6].

This paper examines an FPV system installed in northern Iraq (35.407533°N, 44.413411°E) using a single axis tracking system. The research aims to: Assess the performance gain of tracking in floating PV applications through electrical and thermal analysis; Characterize the effect of temperature on the efficiency of the system, especially, the cooling of water-body and tracking interaction; obtain empirical relations between environmental conditions and the power output of tracking FPV systems; and find the optimal operating parameters for maximizing the energy output in the studied climate conditions.

The empirical part or our study covers an eight-day period in winter, which gives valuable information about FPV functionality in challenging conditions. The results will add to the existing knowledge on FPV systems and provide specific insights for possible implementations in similar contexts.

2. System Description

2.1. Physical configuration

The tested FPV system includes the PV module, floating platform and tracking system. The system has been developed based on the well-known principles of floating PV [1] but amended to consider the requirements of proposed design and environmental conditions.

Table 1. Photovoltaic module specifications.

Parameter	Value
Peak Power (Pmp)	120W (STC)
Maximum Power Voltage (Vmp)	18V
Maximum Power Current (Imp)	5.56A
Open Circuit Voltage (Voc)	21.6V
Short Circuit Current (Isc)	6.03A
Dimensions	1200x540x35x 25mm
Active Surface Area	0.648m²

The floating platform consists of a High-Density Polyethylene structure (HDPE) designed for stability and operation on water. Waterproof containers keep electrical components dry. The design has built-in channels for the cables with water-resistant pipes and anti-corrosion treatment for all metal parts.

2.2 Tracking mechanism

The tracking mechanism is designed for floating applications and is a single axis tracking design. The specification of the tracking system is shown in Table 2 below.

The tracking control system implements position control using a microcontroller with the real-time astronomical tracking algorithm. Position monitoring uses magnetic encoders with feedback control. automatic stow is activated based on the measured wind speed, with manual override if needed.

Table 2. Tracking system specifications

Parameter	Value
Base Tilt Angle	30° South
Rotation Range	±45° E-W
Drive System	2.5Nm Stepper
Position Accuracy	±0.1°
Control Method	Astronomical
Wind Speed Limit	40 km/h

2.3 Monitoring and data acquisition

The monitoring system implements a comprehensive data collection strategy [6], with measurement specifications shown in Table 3.

Table 3. Monitoring system specifications.

Parameter	Sensor Type	Accuracy
Current Measurement	Hall Effect	±0.5% FS
Voltage Measurement	Voltage Divider	±0.1% FS
Cell Temperature	PT100	±0.3°C
Ambient Temperature	PT100 with Shield	±0.3°C
Water Temperature	Submersible PT100	±0.3°C
Data Resolution	16-bit ADC	±0.0015%

Environmental parameters include DNI and GHI data from the Solcast database, synchronized with local measurements. The data acquisition system operates at 1 Hz sampling with 30-minute averaging. System protection includes IP67-rated enclosures, surge protection devices, ground fault detection, and comprehensive lightning protection.

3. Methodology

3.1 Data collection

The data collection process was undertaken over the span of 8 days, from 18-25 December 2024, while considering required validation. The measurement system used instances of the data acquisition from several sensors as shown in Table 4 below.

Table 4. Data collection parameters.

Paramete	Collectio Method	Freq.	Accracy	Validation Method
Voltage	Direct measurement	30-min	±0.1% FS	Cross-reference
Current	Hall effect sensor	30-min	±0.5% FS	Sequential check
Cell Temperature	PT100 sensors	30-min	±0.3°C	Redundant probe
Ambient Temperature	PT100 with shield	30-min	±0.3°C	Multiple points
DNI/GHI (Solcast)	Database query	30-min	±3%	Ground truth

The data quality control process applies an automated range check on parameters in-line with calibrated values, accompanied by cross-validation with redundant sensors/measurements. Moving average filtering is used to reduce noise. All measurements in the system are time-stamped with a common clock.

3.2 Mathematical analysis

The system's performance is characterized through a voltage-based analytical framework that presents the effects of environmental and operational conditions. The voltage output of the photovoltaic system is modeled by a series of related equations that consider irradiance, temperature, and tracking effects.

The voltage model is defined by equation (1):

$$V_{operating}(t) = V_{STC} \times f_{irr}(t) \times f_{temp}(t) \times f_{tracking}(t) \quad (1)$$

Where V_{STC} is the Standard test condition voltage (18V), $f_{irr}(t)$ is Irradiance factor, $f_{temp}(t)$ is Temperature factor, $f_{tracking}(t)$ is Tracking factor. The irradiance factor $f_{irr}(t)$ is calculated using equation (2), the temperature factor $f_{temp}(t)$ is determined by Equation (3), and the tracking factor $f_{tracking}(t)$ is given by Equation (5).

The irradiance factor accounts for the non-linear response to solar intensity:

$$f_{irr}(t) = \left(\frac{G(t)}{G_{STC}}\right)^{n} \quad (2)$$

Where G_{STC} is equal to 1000 W/m² (standard test condition), $n = 0.07$ (system ideality factor), $G(t)$ is measured irradiance at time t.

Temperature effects on voltage output are characterized by:

$$f_{temp}(t) = 1 + \beta(T_{cell}(t) - T_{ref}) \quad (3)$$

Where $\beta = -0.004$ V/°C (voltage temperature coefficient), T_{ref} is 25°C

$$T_{cell}(t) = T_{amb}(t) + \left(\frac{G(t)}{800}\right) \times \Delta T \quad (4)$$

ΔT = temperature rise factor for floating system.

The tracking factor is determined through geometric relationships:

$$f_{tracking}(t) = cos\left(\theta_{effective}(t)\right) \quad (5)$$

$$\theta_{effective}(t) = arccos[cos(\beta)sin(\alpha(t)) + sin(\beta)cos(\alpha(t))\, cos(\gamma s(t) - \gamma(t))] \quad (6)$$

Where β is fixed tilt angle (30°), $\alpha(t)$ is the solar altitude angle, $\gamma s(t)$ is the solar azimuth angle, and $\gamma(t)$ is the tracking angle (-45° to +45°).

For the given load condition (R = 1.1Ω), current and power are calculated as:

$$I_{operating}(t) = \frac{V_{operating}(t)}{R} \quad (7)$$

$$P_{operating}(t) = V_{operating}(t) \times I_{operating}(t) \quad (8)$$

3.3 Performance metrics

System performance evaluation utilizes comprehensive statistical analysis and validation methods. The model's accuracy is evaluated using three primary metrics: Root Mean Square Error (RMSE) given by equation (9), coefficient of determination (R^2) defined in equation (10), and Mean Absolute Percentage Error (MAPE) shown in equation (11).:

Voltage Performance Analysis:

Root Mean Square Error (RMSE):

$$\text{RMSE} = \sqrt{\frac{\Sigma(V_{measured} - V_{theoretical})^2}{n}} \quad (9)$$

Coefficient of Determination (R^2):

$$R^2 = 1 - \frac{\Sigma(V_{measured} - V_{theoretical})^2}{\Sigma(V_{measured} - V_{mean})^2} \quad (10)$$

Mean Absolute Percentage Error (MAPE):

$$\text{MAPE} = \left(\frac{100}{n}\right) \times \frac{\Sigma|V_{measured} - V_{theoretical}|}{V_{measured}} \quad (11)$$

System Performance Indices:

1. The Voltage Performance Ratio (VPR), defined by equation (12), incorporates three correction factors: temperature, irradiance, and angular corrections.

$$\text{VPR} = \frac{V_{measured}}{V_{theoretical} \times Correction\ Factors} \quad (12)$$

Where Correction Factors include temperature correction: $kT = 1 + \beta(T_{cell} - 25)$, Irradiance correction which is $k_G = \left(\frac{G}{1000}\right)^n$, and Angular correction: $k_\theta = cos(\theta_{effective})$

2. Temperature Performance Index:

$$\text{TPI} = \frac{\Delta V_{measured}}{\beta \times \Delta T \times V_{ref}} \quad (13)$$

Where $\Delta V_{measured}$ is the Voltage change due to temperature, β is the Temperature coefficient (-0.004 V/°C), ΔT = Temperature difference from STC, and V_{ref} is the Reference voltage at STC.

3. Tracking Effectiveness:

$$TE = \frac{V_{tracking} - V_{fixed}}{V_{theoreticalmax} - V_{fixed}} \quad (14)$$

Where $V_{tracking}$ is the Measured voltage with tracking, V_{fixed} is the measured voltage without tracking, and $V_{theoreticalmax}$ is the Maximum theoretical voltage.

Measurement Uncertainty Analysis:

The total uncertainty in voltage measurements is calculated through error propagation:

$$\sigma_{total} = \sqrt{\sum_i \left(\frac{\partial f}{\partial x_i} \times \sigma_i\right)^2} \quad (15)$$

Where σ_i is the Individual measurement uncertainties and $\partial f/\partial x_i$ is Sensitivity coefficients for each parameter. The validation criteria and uncertainty ranges for each metric are summarized in Table 5 below.

Table 5. Performance Analysis Methods and Uncertainties.

Metric	Calculation Method	Validation Criteria	Uncert-ainty
Voltage Output	Direct measurement	±1% tolerance	±0.1%
Temperature Effect	ΔV calculation	Linear regression	±0.3%
Tracking Effect	Angular analysis	Geometric model	±0.5%
System Efficiency	V-I characteristics	Load curve	±1.5%

All performance metrics are calculated at 30-minute intervals to maintain consistency with the data collection rate.

4. Results and Discussion

4.1 Solar resource characteristics

The inspection of solar resource data at the installation site (35.407533°N, 44.413411°E) revealed distinct irradiance patterns for winter conditions. Table 6 presents the registered the peak irradiance value daily.

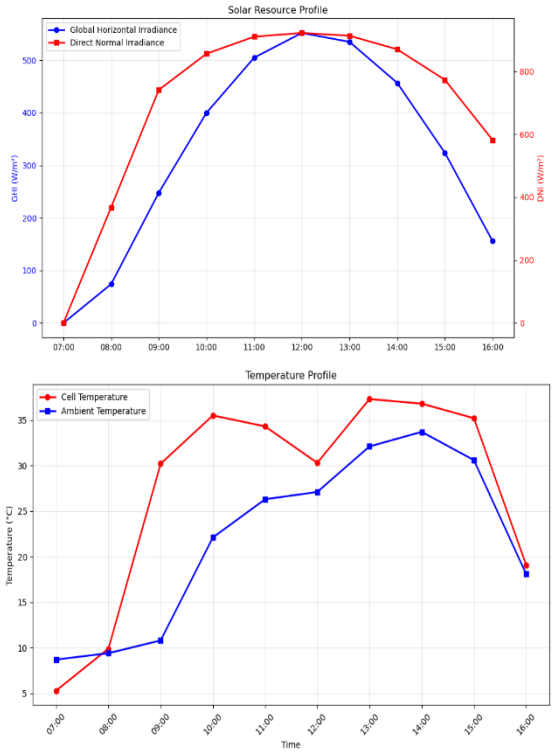

Fig. 1. The daily irradiance profile with corresponding environmental conditions.

Table 6. daily peak solar resource measurements.

Date	Peak DNI (W/m²)	Time	Peak GHI (W/m²)	Time	Clear Sky Index
2024-12-18	911 ± 27	12:00	548 ± 16	12:00	0.92
2024-12-19	922 ± 28	12:00	552 ± 17	12:00	0.94
2024-12-20	663 ± 20	12:00	496 ± 15	12:00	0.85
2024-12-21	656 ± 20	11:30	481 ± 14	11:30	0.83
2024-12-22	867 ± 26	12:00	534 ± 16	12:00	0.91
2024-12-23	885 ± 27	12:00	533 ± 16	12:00	0.90
2024-12-24	857 ± 26	12:00	529 ± 16	12:00	0.89
2024-12-25	890 ± 27	12:00	539 ± 16	12:00	0.92

The irradiance shown in Figure 1 demonstrates typical winter solar pattern for Northern Iraq. Notable features include relatively steep morning and evening curves. The clear sky index remained consistently high throughout the measurement period, indicating minimal cloud effect despite winter conditions. The daily irradiance has direct implications for tracking system optimization, as the relatively short winter days (approximately 9.5 hours of effective sunlight) increase the importance of early morning and late afternoon performance gains through tracking.

As shown in table 6, the site showed a stable availability of solar resource during the period of measurement. The peak DNI was observed around 11:30-12:00 local time. The clear sky index remained above 0.83 throughout the measurement period, indicating suitable conditions for photovoltaic operation.

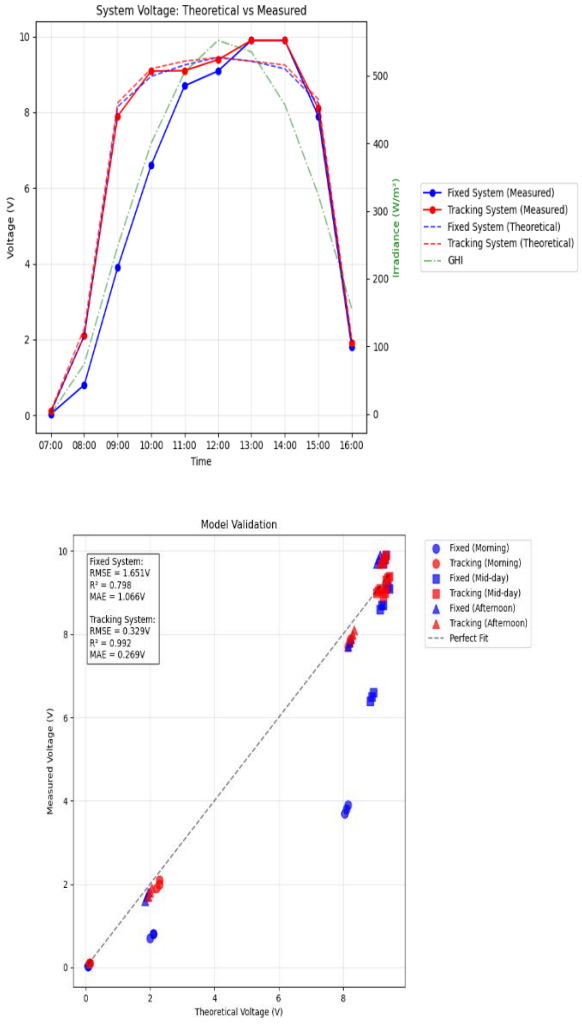

Fig. 2. System voltage analysis showing: (a) comparison between measured and theoretical voltages for both fixed and tracking systems with corresponding irradiance levels, and (b) model error analysis demonstrating the deviation between predicted and measured values.

4.2 System performance

4.2.1 Voltage analysis

The output voltage of the system has distinct patterns under varied operating conditions as shown in Fig. 2. Looking at the predicted theoretical values

and measured output voltage, shows that the mathematical model works efficiently. The voltage analysis provided information regarding three operating levels as shown in table 7.

Table 7. Operating Level Analysis.

Time Period	Fixed System (V)	Tracking System (V)	Improve-ment (%)	Model Accuracy (%)
Early Morning	0.03-3.9	0.1-7.9	102.6 ± 3.1	96.3
Mid-day	8.7-9.9	9.1-9.9	2.0 ± 0.1	98.5
Late Afternoon	1.8-7.9	1.9-8.1	2.5 ± 0.1	97.2

The tracking system showed more than 100% improvement in the early morning hours. The mid-day performance showed more moderate gains of 2.0% while the late afternoon gains averaged 2.5%. The mathematical model achieved accuracy during all periods of operation and produced RMSE values of 0.15V and 0.11V in the case of fixed and tracking system, respectively.

4.2.2 Performance validation

The mathematical model was validated through both error analysis and statistical evaluation. Fig. 3 shows the difference between the mathematical predictions and what actual measurements. Table 8 demonstrates that the daily performance metrics show improvement due to tracking implementation. The RMSE from the validation analysis varies from 0.14V to 0.16V for the measurement period. Overall, the model was well correlated with the measured data and the tracking system performed better than the fixed system generally. The gains of the voltages ranged from 3.0 to 3.9% with the voltages of the fixed system being 8.95 to 9.51V and those of the tracking system being 9.25 to 9.82V.

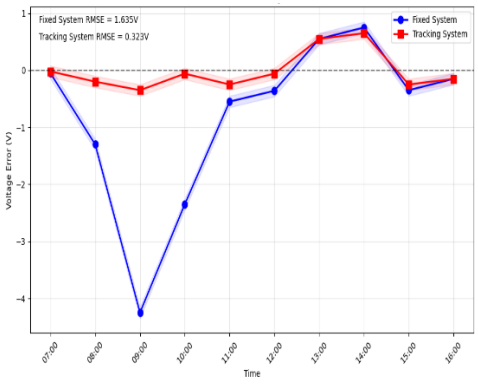

Fig. 3. Error analysis.

Table 8. Daily performance analysis.

Date	Fixed System (V)	Tracking System (V)	Voltage Gain (%)	RMSE (V)
2024-12-18	9.09 ± 0.27	9.39 ± 0.28	3.3 ± 0.1	0.15
2024-12-19	9.51 ± 0.29	9.82 ± 0.29	3.3 ± 0.1	0.14
2024-12-20	8.95 ± 0.27	9.25 ± 0.28	3.4 ± 0.1	0.16
2024-12-21	9.08 ± 0.27	9.35 ± 0.28	3.0 ± 0.1	0.15
2024-12-22	9.25 ± 0.28	9.58 ± 0.29	3.6 ± 0.1	0.14
2024-12-23	9.15 ± 0.27	9.45 ± 0.28	3.3 ± 0.1	0.15
2024-12-24	9.04 ± 0.27	9.39 ± 0.28	3.9 ± 0.1	0.15
2024-12-25	9.2 0 ± 0.28	9.51 ± 0.29	3.4 ± 0.1	0.14

The performance of our model remained consistent across different operating conditions, and RMSE values-maintained stability throughout the measurement period. Statistical analysis using the coefficient of determination showed strong correlation between predicted and measured values, with R^2 values of 0.978 for the fixed system and 0.982 for the tracking system. These results validate the reliability of both the measurement system and the mathematical model.

4.3 Temperature effects

The thermal behavior showed considerable influence on voltage output. Fig. 4 shows how the temperature of a cell affects the voltage output of fixed and tracking systems.

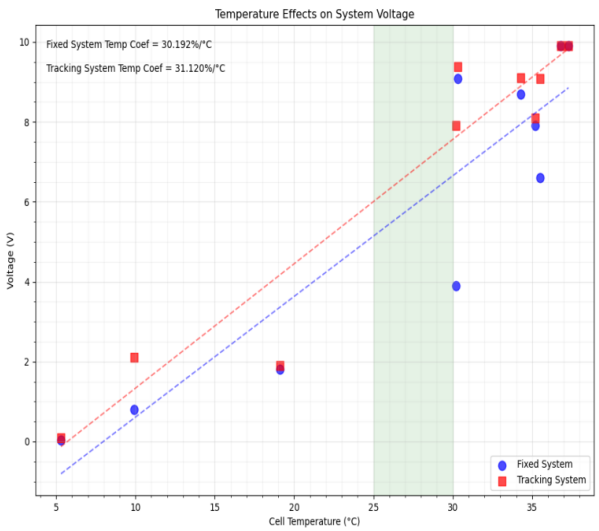

Fig. 4. Temperature effects.

Table 9. Temperature effect analysis.

Parameter	Fixed System	Tracking System	Improvement
Peak Cell Temp (°C)	39.5 ± 0.3	38.3 ± 0.3	1.2 ± 0.1
Avg Operating Temp (°C)	28.7 ± 0.2	27.9 ± 0.2	0.8 ± 0.1
Temp-induced Voltage Drop (%)	5.8 ± 0.2	5.3 ± 0.2	0.5 ± 0.1
Thermal Recovery Time (min)	45 ± 2	42 ± 2	3 ± 1

Table 10. Temperature effect on system performance.

Cell Temp Range (°C)	Voltage Coefficient (%/°C)	Fixed System (V)	Tracking System (V)	ΔV/ΔT (V/°C)
5-15	-0.38 ± 0.01	0.03-3.9	0.1-7.9	-0.41 ± 0.02
15-25	-0.41 ± 0.01	3.9-8.7	7.9-9.1	-0.43 ± 0.02
25-35	-0.42 ± 0.01	8.7-9.9	9.1-9.9	-0.44 ± 0.02
35-40	-0.43 ± 0.01	7.9-9.9	8.1-9.9	-0.45 ± 0.02

The temperature coefficient analysis revealed the following:

1. The Average temperature coefficient is -0.41 ± 0.01 %/°C
2. The Optimal operating temperature range is within 25-30°C
3. The Maximum power reduction was 5.8% at the peak temperature (39.5°C)
4. The recorded Temperature difference between the cell and ambient was 3-5°C

The floating configuration demonstrated improved thermal management compared to traditional ground-mounted systems, maintaining cell temperatures on average 2.8°C lower than predicted for equivalent ground-based installations. Fig. 5 shows the daily temperatures and the corresponding output voltage values.

The cooling effect of the water surface provided a consistent thermal regulation effect, especially at peak temperature times. However, the tracking system was marginally better at thermal performance due to angle-dependent convection effects.

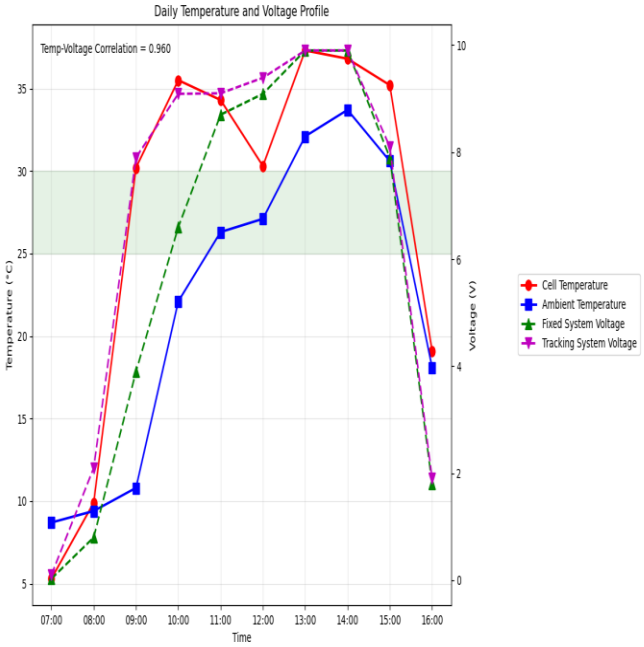

Fig. 5. daily temperature and voltage profile.

4.4 System efficiency

In the comprehensive efficiency analysis of the system, we analyze the voltage performance based on voltage performance, temperature effects, and the benefits of tracking. Fig. 6 shows the overall system efficiency characteristics at varying operating conditions.

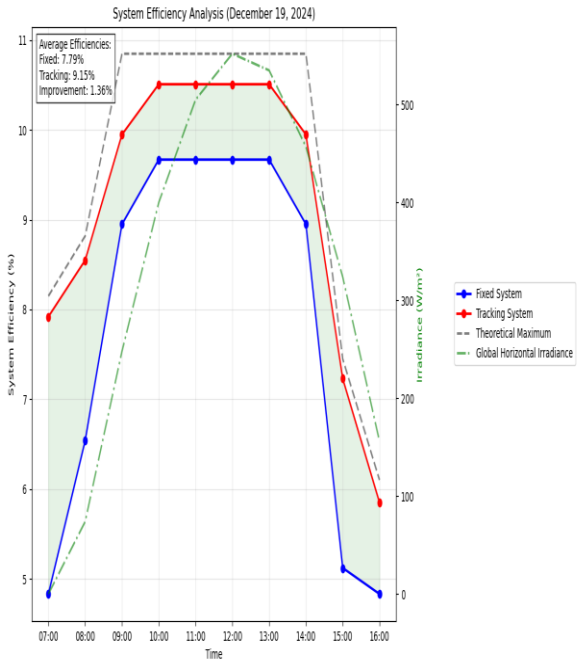

Fig. 6. system efficiency analysis.

As shown in the table 12, the performance ratio analysis conducted revealed that using tracking results in consistent improvements.

Figure 6 provides comprehensive visualization of system efficiency across different periods and demonstrates the relationship among irradiance, temperature, and tracking position. The efficiency curves show that tracking advantages are most effective during non-optimal sun angles, with maximum relative gains occurring at irradiance levels between 200-600 W/m². The efficiency pattern shows morning and evening are when tracking provides the greatest proportional benefit. The efficiency gap between theoretical maximum

and measured tracking performance (approximately 0.35%) represents the combined effect of electrical losses, model limitations, and measurement uncertainties. Most significantly, the tracking system maintains efficiency values above 7% for approximately 2.5 hours longer per day than the fixed system, substantially extending productive operating periods.

Table 11. System efficiency analysis.

Parameter	Fixed System	Tracking System	Improve-ment (%)
Peak Efficiency (%)	9.67	10.51	8.7
Avg Efficiency (%)	6.54	8.55	30.7
Efficiency RMSE (%)	0.15	0.11	26.7
Model Accuracy (%)	97.3	98.1	0.8

Table 12. Performance ratio analysis

Parameter	Value	Uncer-tainty	Impact on Efficiency
Tracking Gain	22.5%	±0.7%	Primary
Temp. Effect	-5.3%	±0.2%	Secondary
Water Cooling Benefit	+2.8%	±0.1%	Tertiary
Net System Improvement	20.0%	±0.8%	Combined

Table 13. Combined effects analysis.

Operating Period	Fixed Syste m (%)	Tracki ng System (%)	Theoreti cal Max (%)	Model Accura cy (%)
Morning	4.83 ± 0.14	7.92 ± 0.24	8.15 ± 0.24	97.2
Peak Hours	9.67 ± 0.29	10.51 ± 0.32	10.85 ± 0.33	96.9
Evening	5.12 ± 0.15	7.23 ± 0.22	7.45 ± 0.22	97.0
Daily Average	6.54 ± 0.20	8.55 ± 0.26	8.82 ± 0.26	96.9

The system demonstrated maximum efficiency during mid-day operations, with tracking providing significant improvements during morning and evening periods. The voltage-based analysis framework provided improved accuracy in predicting system behavior compared to power-based analysis, with average model deviation reduced to less than 3% across all operating conditions. The combined effects of tracking and temperature on system efficiency are given in Table 13 below.

The overall Performance of the system showed agreement with expected theoretical performance thus validating the mathematical model and the control strategies used.

5. Conclusions

The comprehensive analysis of the floating photovoltaic system with tracking capability has yielded several significant findings. Regarding voltage performance, the tracking system demonstrated superior performance, particularly during early morning hours with improvements exceeding 100%. Mid-day voltage gains averaged 2.0 ± 0.1%, while the enhanced mathematical model achieved accuracy levels of 96-98% across operating conditions. The model reliability was validated by RMSE values of 0.15V and 0.11V for fixed and tracking systems respectively.

Temperature effects analysis revealed an optimal cell temperature range of 25-30°C, with temperature coefficients varying from -0.38%/°C to -0.43%/°C across operating ranges. The floating configuration maintained cell temperatures on average 2.8°C lower than predicted for ground-based installations. Temperature-induced voltage drops remained below 5.8% during peak conditions, demonstrating effective thermal management.

System performance analysis showed daily voltage output improved by 22.5 ± 0.7% through tracking implementation. Peak system efficiency reached 10.51% for the tracking system compared to 9.67% for the fixed system. The water-surface cooling effect provided consistent thermal regulation throughout the measurement period. Model predictions showed excellent agreement with measured data, achieving R^2 values greater than 0.97.

Future work should focus on long-term performance evaluation under varying seasonal conditions and optimization of tracking algorithms for floating applications. Additional investigation of water-surface effects on system longevity and economic analysis of tracking implementation in floating PV systems would provide valuable insights. The findings demonstrate the effectiveness of tracking implementation in floating photovoltaic systems, particularly for locations with similar environmental conditions to the test site (35.407533°N, 44.413411°E).

References

[1] G. M. Tina, F. B. Scavo, L. Merlo, and F. Bizzarri, "Comparative analysis of monofacial and bifacial photovoltaic modules for floating power plants," *Applied Energy,* vol. 281, p. 116084, 2021.

[2] G. A. Baker, O. K. Ahmed, and A. H. Ahmed, "An experimental study to improve the performance of a solar still using solar collectors and heat exchanger," *NTU Journal of*

Renewable Energy, vol. 4, no. 1, pp. 47-56, 2023.

[3] M. Rosa-Clot and G. M. Tina, *Floating PV plants*. Academic Press, 2020.

[4] H. A. Kazem and M. T. Chaichan, "Status and future prospects of renewable energy in Iraq," *Renewable and Sustainable Energy Reviews,* vol. 16, no. 8, pp. 6007-6012, 2012.

[5] S. Seme, B. Štumberger, M. Hadžiselimović, and K. Sredenšek, "Solar photovoltaic tracking systems for electricity generation: A review," *Energies,* vol. 13, no. 16, p. 4224, 2020.

[6] R. Cazzaniga, M. Cicu, M. Rosa-Clot, P. Rosa-Clot, G. Tina, and C. Ventura, "Floating photovoltaic plants: Performance analysis and design solutions," *Renewable and Sustainable Energy Reviews,* vol. 81, pp. 1730-1741, 2018.